We are IntechOpen, the world's leading publisher of Open Access books Built by scientists, for scientists

4,800
Open access books available

122,000
International authors and editors

135M
Downloads

Our authors are among the

154
Countries delivered to

TOP 1%
most cited scientists

12.2%
Contributors from top 500 universities

WEB OF SCIENCE™

Selection of our books indexed in the Book Citation Index in Web of Science™ Core Collection (BKCI)

Interested in publishing with us?
Contact book.department@intechopen.com

Numbers displayed above are based on latest data collected.
For more information visit www.intechopen.com

17

A Sensor Classification Strategy for Robotic Manipulators

Miguel F. M. Lima [1], J. A. Tenreiro Machado [2] and António Ferrolho [3]
[1,3] *Dept. of Electrical Engineering, School of Technology, Polytechnic Institute of Viseu, Portugal, {lima, antferrolho}@mail.estv.ipv.pt*
[2] *Dept. of Electrical Engineering, Institute of Engineering, Polytechnic Institute of Porto, Portugal, jtm@isep.ipp.pt*

1. Introduction

In practice the robotic manipulators present some degree of unwanted vibrations. The advent of lightweight arm manipulators, mainly in the aerospace industry, where weight is an important issue, leads to the problem of intense vibrations. On the other hand, robots interacting with the environment often generate impacts that propagate through the mechanical structure and produce also vibrations.
In order to analyze these phenomena a robot signal acquisition system was developed. The manipulator motion produces vibrations, either from the structural modes or from end-effector impacts. The instrumentation system acquires signals from several sensors that capture the joint positions, mass accelerations, forces and moments, and electrical currents in the motors. Afterwards, an analysis package, running off-line, reads the data recorded by the acquisition system and extracts the signal characteristics.
Due to the multiplicity of sensors, the data obtained can be redundant because the same type of information may be seen by two or more sensors. Because of the price of the sensors, this aspect can be considered in order to reduce the cost of the system. On the other hand, the placement of the sensors is an important issue in order to obtain the suitable signals of the vibration phenomenon. Moreover, the study of these issues can help in the design optimization of the acquisition system. In this line of thought a sensor classification scheme is presented.
Several authors have addressed the subject of the sensor classification scheme. White (White, 1987) presents a flexible and comprehensive categorizing scheme that is useful for describing and comparing sensors. The author organizes the sensors according to several aspects: measurands, technological aspects, detection means, conversion phenomena, sensor materials and fields of application. Michahelles and Schiele (Michahelles & Schiele, 2003) systematize the use of sensor technology. They identified several dimensions of sensing that represent the sensing goals for physical interaction. A conceptual framework is introduced that allows categorizing existing sensors and evaluates their utility in various applications. This framework not only guides application designers for choosing meaningful sensor

subsets, but also can inspire new systems and leads to the evaluation of existing applications.
Today's technology offers a wide variety of sensors. In order to use all the data from the diversity of sensors a framework of integration is needed. Sensor fusion, fuzzy logic, and neural networks are often mentioned when dealing with problem of combing information from several sensors to get a more general picture of a given situation. The study of data fusion has been receiving considerable attention (Esteban et al., 2005; Luo & Kay, 1990). A survey of the state of the art in sensor fusion for robotics can be found in (Hackett & Shah, 1990). Henderson and Shilcrat (Henderson & Shilcrat, 1984) introduced the concept of logic sensor that defines an abstract specification of the sensors to integrate in a multisensor system.
The recent developments of micro electro mechanical sensors (MEMS) with unwired communication capabilities allow a sensor network with interesting capacity. This technology was applied in several applications (Arampatzis & Manesis, 2005), including robotics. Cheekiralla and Engels (Cheekiralla & Engels, 2005) propose a classification of the unwired sensor networks according to its functionalities and properties.
This paper presents a development of a sensor classification scheme based on the frequency spectrum of the signals and on a statistical metrics.
Bearing these ideas in mind, this paper is organized as follows. Section 2 describes briefly the robotic system enhanced with the instrumentation setup. Section 3 presents the experimental results. Finally, section 4 draws the main conclusions and points out future work.

2. Experimental platform

The developed experimental platform has two main parts: the hardware and the software components (Lima et al., 2005). The hardware architecture is shown in Fig. 1. Essentially it is made up of a robot manipulator, a personal computer (PC), and an interface electronic system.
The interface box is inserted between the robot arm and the robot controller, in order to acquire the internal robot signals; nevertheless, the interface captures also external signals, such as those arising from accelerometers and force/torque sensors. The modules are made up of electronic cards specifically designed for this work. The function of the modules is to adapt the signals and to isolate galvanically the robot's electronic equipment from the rest of the hardware required by the experiments.
The software package runs in a Pentium 4, 3.0 GHz PC and, from the user's point of view, consists of two applications: the acquisition application and the analysis package. The acquisition application is a real time program for acquiring and recording the robot signals.
After the real time acquisition, the analysis package processes the data off-line in two phases, namely, pre-processing and processing. The preprocessing phase consists of the signal selection in time, and their synchronization and truncation. The processing stage implements several algorithms for signal processing such as the auto and cross correlation, and Fourier transform (FT).

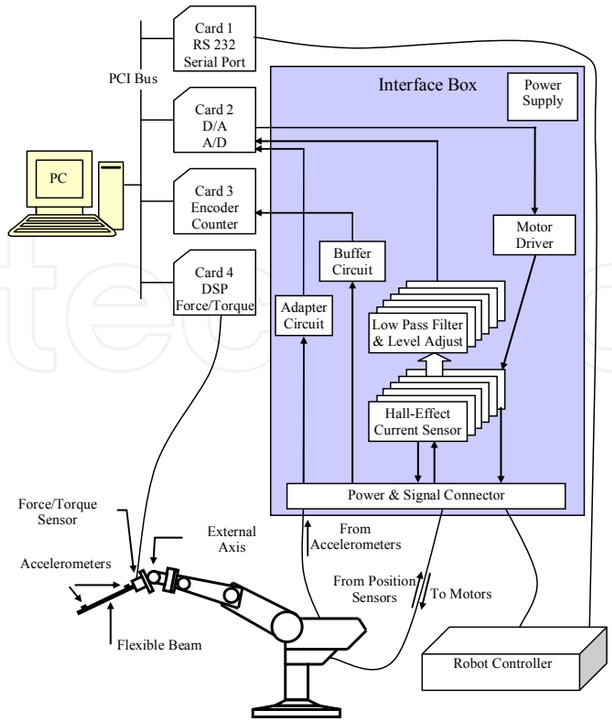

Fig. 1. Block diagram of the hardware architecture

3. Experimental results

According to the platform described in Section 2 a set of experiments is developed. Based on the signals captured from the robot this section presents several results obtained both in the time and frequency domains.

In the experiments a flexible link is used that consists of a long and round flexible steel rod clamped to the end-effector of the manipulator. In order to analyze the impact phenomena in different situations two types of beams are used. Their physical properties are shown in Table 1. The robot motion is programmed in a way such that the rods move against a rigid surface. Figure 2 depicts the robot with the flexible link and the impact surface.

During the motion of the manipulator the clamped rod is moved by the robot against a rigid surface. An impact occurs and several signals are recorded with a sampling frequency of f_s = 500 Hz. The signals come from several sensors, such as accelerometers, force and torque sensor, position encoders, and current sensors.

In order to have a wide set of signals captured during the impact of the rods against the vertical screen thirteen trajectories were defined. Those trajectories are based on several points selected systematically in the workspace of the robot, located on a virtual Cartesian coordinate system (see Fig. 3). This coordinate system is completely independent from that used on the measurement system. For each trajectory the motion of the robot begins in one of these points, moves against the surface and returns to the initial point. A parabolic profile was used for the trajectories.

Fig. 2. Steel rod impact against a rigid surface

Characteristics	Thin rod	Gross rod
Material	Steel	Steel
Density [kg m^{-3}]	4.34×10^3	4.19×10^3
Mass [kg]	0.107	0.195
Length [m]	0.475	0.475
Diameter [m]	5.75×10^{-3}	7.9×10^{-3}

Table 1. Physical properties of the flexible beams

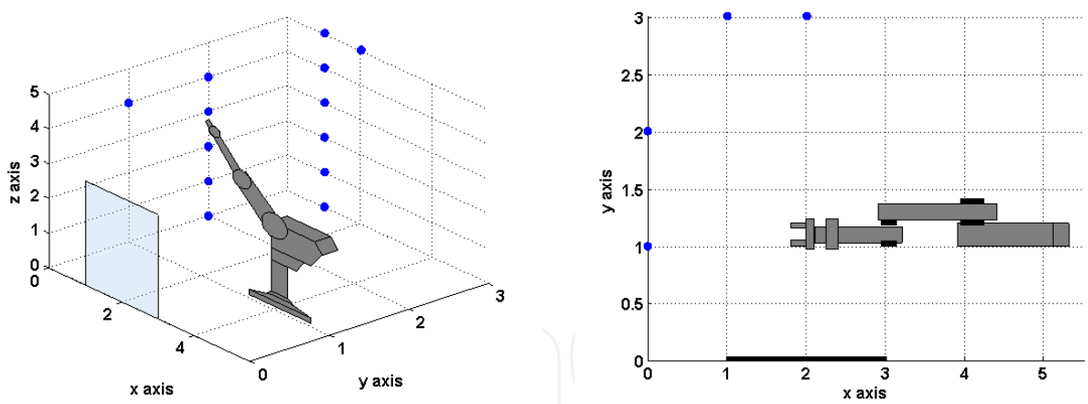

Fig. 3. Schematic representation 3D (left) and 2D (right) of the robot and the impact surface on the virtual cartesian coordinate system

3.1 Analysis in the time domain

Figures 4 to 7 depict some of the signals corresponding to the cases: (*i*) without impact, (*ii*) the impact of the rod on a gross screen and (*iii*) the impact of the rod on a thin screen using either the thin or the gross rod.

In this chapter only the most relevant signals are depicted, namely the forces and moments at the gripper sensor, the electrical currents of the robot's axes motors, and the rod accelerations. The signals present clearly a strong variation at the instant of the impact that occurs, approximately, at t = 3 s. Consequently, the effect of the impact forces (Fig. 4 left)

and moments (Fig. 4 right) is reflected in the current required by the robot motors (Fig. 6). Moreover, as expected, the amplitudes of forces due to the gross screen (case ii) are higher than those corresponding to the thin screen (case iii). On the other hand, the forces with the gross rod (Fig. 4 right) are higher than those that occur with the thin rod (Fig. 4 left). The torques present also an identical behavior in terms of its amplitude variation for the tested conditions (see Fig. 5).

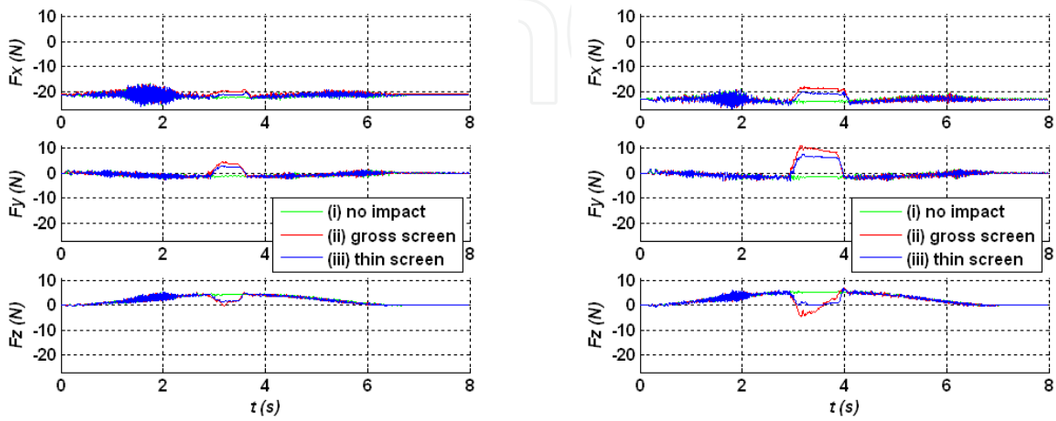

Fig. 4. Forces { F_x, F_y, F_z } at the gripper sensor: thin rod (left); gross rod (right)

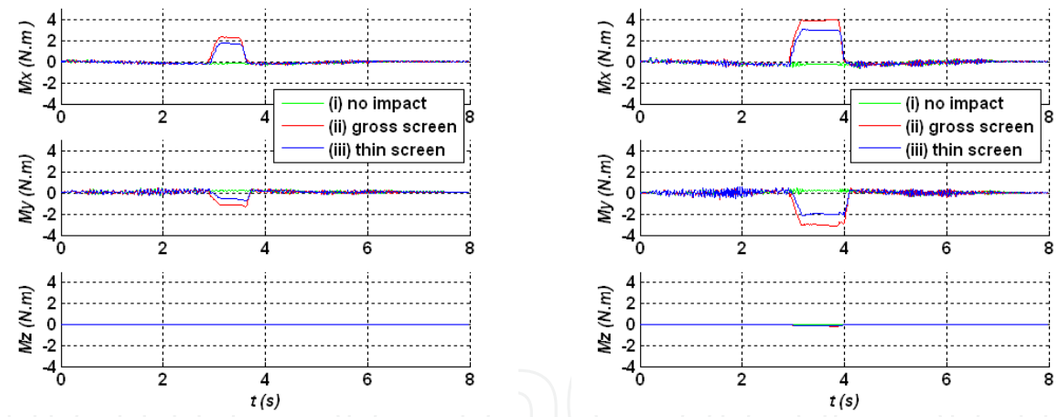

Fig. 5. Moments { M_x, M_y, M_z } at the gripper sensor: thin rod (left); gross rod (right)

Figure 7 presents the accelerations at the rod free-end (accelerometer 1), where the impact occurs, and at the rod clamped-end (accelerometer 2). The amplitudes of the accelerometers signals are higher near the rod impact side. Furthermore, the values of the accelerations obtained for the thin rod (Fig 7 left) are higher than those for the gross rod (Fig 7 right), because the thin rod is more flexible.

3.2 Analysis in the frequency domain

Figures 8 and 9 show, as examples, the amplitude of the Fast Fourier Transform (FFT), of two signals captured during the same impact trajectory. These figures illustrate the different

behaviors of the spectrum, depending on the signal in study. All the signals of the trajectories set referred previously were studied, but only the most relevant are depicted.

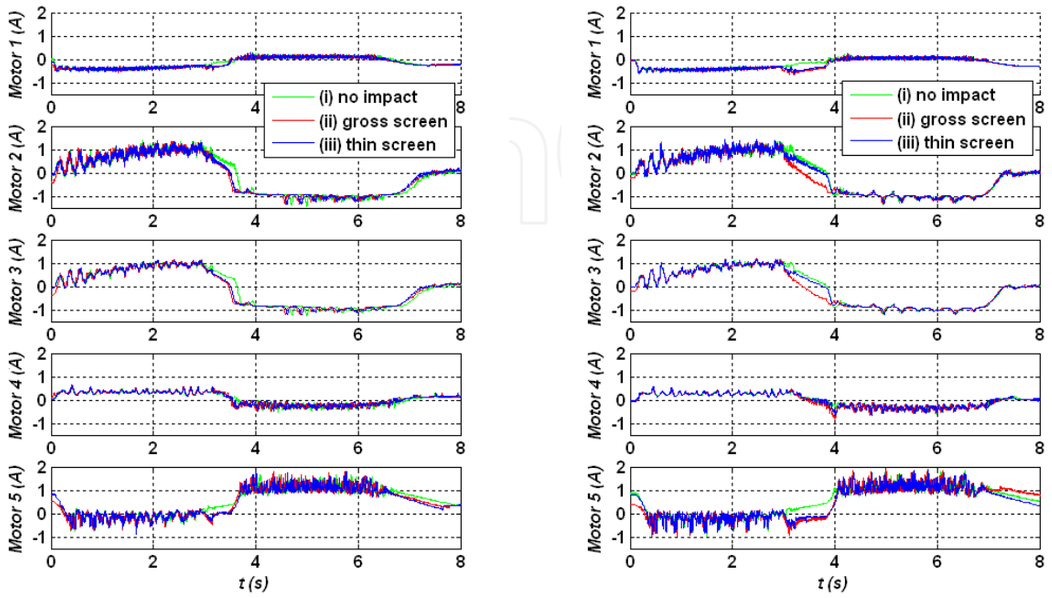

Fig. 6. Electrical currents { I_1, I_2, I_3, I_4, I_5 } of the robot's axes motors: thin rod (left); gross rod (right)

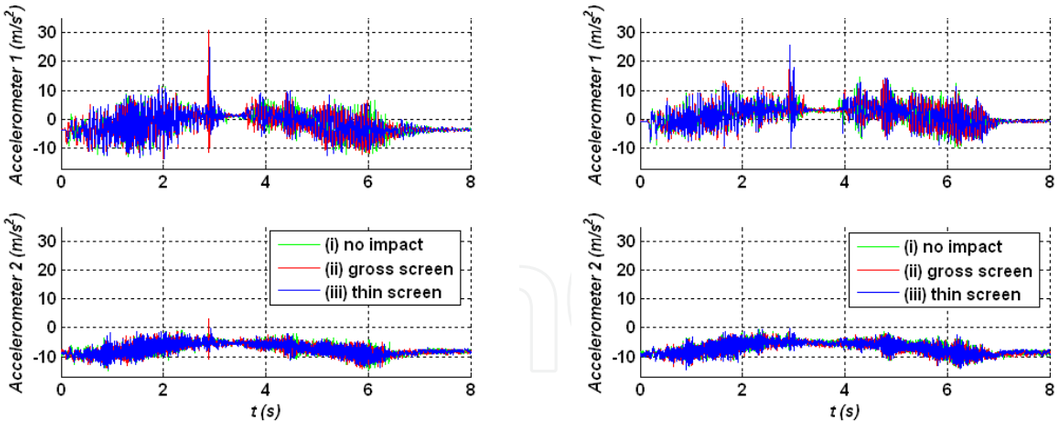

Fig. 7. Rod accelerations { A_1, A_2 }: thin rod (left); gross rod (right)

In order to examine the behavior of the FT signal, in a systematic way, a trendline was superimposed over the spectrum over, at least, one decade. The trendline is based on the power law approximation (Lima et al., 2006).

$$\left|\mathrm{F}\left\{f(t)\right\}\right| \approx c\omega^{m} \tag{1}$$

where F is the FT of the signal, $c \in \Re$ is a constant that depends on the amplitude, ω is the frequency, and $m \in \Re$ is the slope.

For each type of signal, the frequency interval was defined approximately in the middle range of the frequency content of the signal.

Figure 8 shows the FFT amplitude of the electrical current of the axis 3 motor that occurs in the case of impact with the thin rod. A trendline was calculated, and superimposed to the signal (case ii), with slope $m = -1.31$. The others current signals were studied, revealing also an identical behavior in terms of its spectrum spread, both under impact and no impact conditions, either for the thin rod or the gross rod. The spectrum was approximated by trendlines in a frequency range larger than one decade.

According to the robot manufacturer specifications (Robotec, 1996) the loop control of the robot has a cycle time of $t_c = 10$ ms. This fact is observed approximately at the fundamental ($f_c = 100$ Hz) and multiple harmonics in all spectra of motor currents.

The FFT amplitudes of the axes positions signals were studied (Lima et al., 2007), revealing also a behavior similar to the electrical current in terms of the spectrum spread for the tested conditions (impact, no impact, thin rod and gross rod).

Figure 9 shows the FFT amplitude of the F_z force (case *i*) due to the impact with the thin rod. This spectrum is not so well defined in a large frequency range. Nevertheless, the spectrum was approximated by a trendline in a frequency range of approximately one decade in order to get a systematic method of comparison. The trendline has a slope of $m = -0.13$.

The torques and accelerations signals were studied also for the distinct test conditions, namely: impact, no impact, thin rod and gross rod. Their FFT amplitudes revealed also an identical behavior in terms of its spectrum spread for the tested conditions.

Whereas the trendlines used for the electrical currents and position signals FT seem appropriate, the same technique used for the forces/moments and acceleration signals is questionable. However, in spite of this, trendlines were used for all FT signals in order to obtain comparable units. In fact, the purpose of this research is to establish a relationship between signals of the same system based on the spectrum behavior.

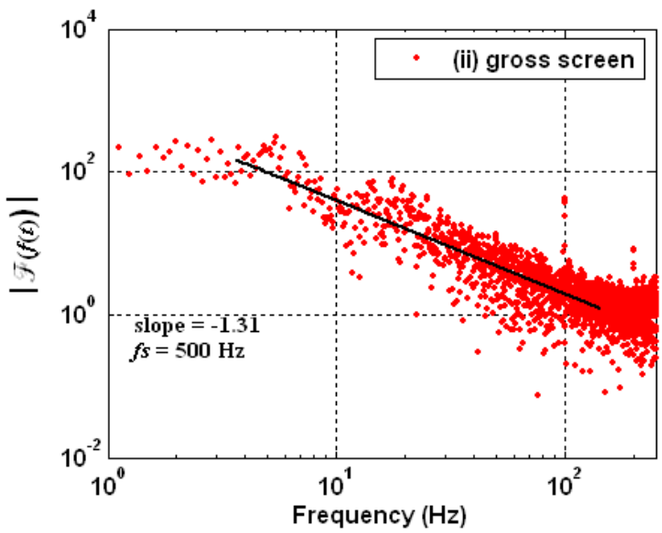

Fig. 8. Spectrum of the axis 3 motor current I_3 for the thin rod

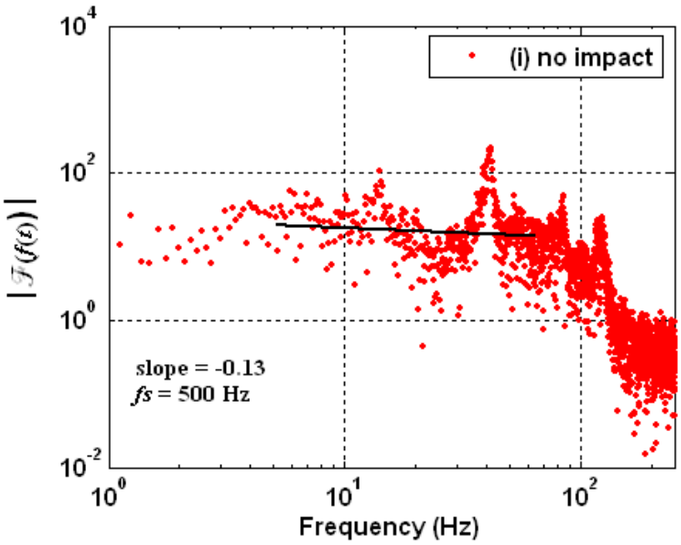

Fig. 9. Spectrum of the F_z force for the thin rod

3.3 Analysis of the spectrum trendlines slopes

Based on the several values of the spectrum trendlines slopes several statistics can be performed. During each trajectory of the robot eighteen signals were captured. For each trajectory there are three cases: (*i*) without impact, (*ii*) the impact of the rod on a gross screen, and (*iii*) the impact of the rod on a thin screen. As referred before, thirteen trajectories were defined. Additionally, the same trajectories were executed with the thin rod and with the gross rod. These samples lead to a population of 1404 slope values.

A box plot provides a visual summary of many important aspects of a data distribution. It indicates the median, upper and lower quartile, upper and lower adjacent values (whiskers), and the outlier individual points. Figure 10 shows a box plot of the spectrum trendlines slopes for the three cases of the thin rod impact, namely: (*i*) without impact, (*ii*) the impact of the rod on a gross screen, and (*iii*) the impact of the rod on a thin screen. Moreover, Fig. 11 depicts the respective interquartile range (IQR) versus the median. The IQR is obtained by subtracting the lower (first) quartile value from the upper (third) quartile value.

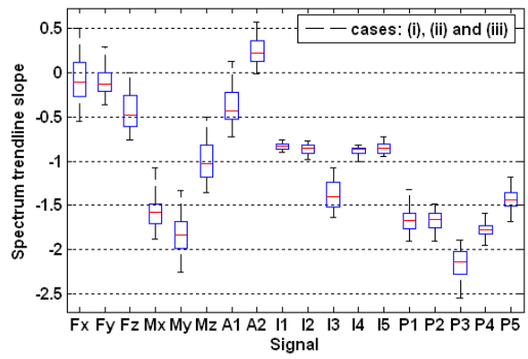

Fig. 10. Statistics of spectrum trendlines slopes for all the cases (*i*, *ii*, *iii*) using the thin rod

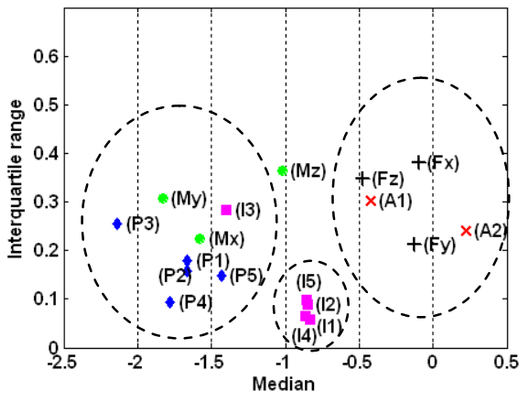

Fig. 11. IQR *versus* median for all the cases (*i*, *ii*, *iii*) using the thin rod

The IQR is a robust way of describing the dispersion of the data. From Fig. 11 three groups of signals can be defined. The ellipses depicted in the chart represent these groups. The forces $\{F_x, F_y, F_z\}$ and the accelerations $\{A_1, A_2\}$ signals are located close to each other. Positions $\{P_1, P_2, P_3, P_4, P_5\}$, moments $\{M_x, M_y\}$, and I_3 signals are located on the left side of the Fig. 11. Finally, the other electrical currents $\{I_1, I_2, I_4, I_5\}$ are situated in the middle of the chart and near each other. It rests the M_z signal that apparently is alone.

Figures 12 and 13 show the same statistic analysis described previously, but now for the gross rod. In Fig. 13 again three groups of signals can be defined. One groups the $\{F_x, F_y, F_z, A_1, A_2\}$ signals, and the second is formed of the $\{I_1, I_2, I_4, I_5\}$ signals. The third group consists of the $\{P_1, P_2, P_3, P_4, P_5, M_x, M_y, M_z, I_3\}$ signals. Comparing with the thin rod case, it can be seen that now the M_z signal joined the group of "torques and positions".

Finally, figures 14 to 15 depict the statistics of the overall spectrum trendlines slopes, considering the data for the thin and gross rods. Three groups are observed again: the group of "positions and torques", the group of "currents" and the group of "forces and accelerations". As can be seen the I_3 signal continues to remain in the same group of "positions and torques". A deeper insight into the nature of this feature must be envisaged to understand the behavior of the I_3 signal.

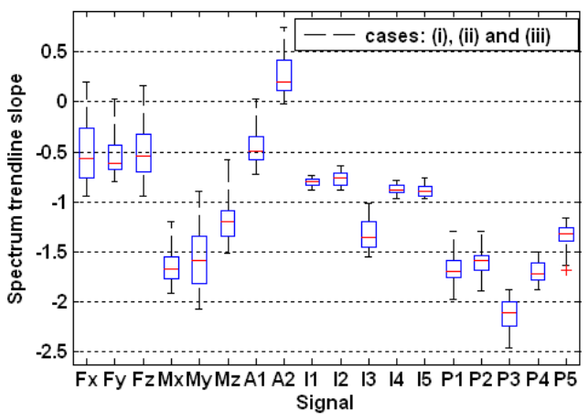

Fig. 12. Statistics of spectrum trendlines slopes for all the cases (*i*, *ii*, *iii*) using the gross rod

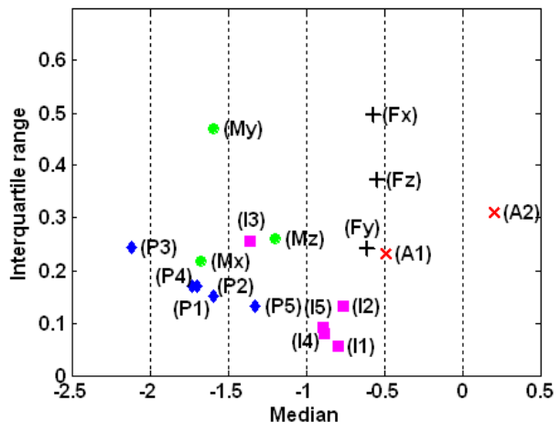

Fig. 13. IQR *versus* median for all the cases (*i, ii, iii*) using the gross rod

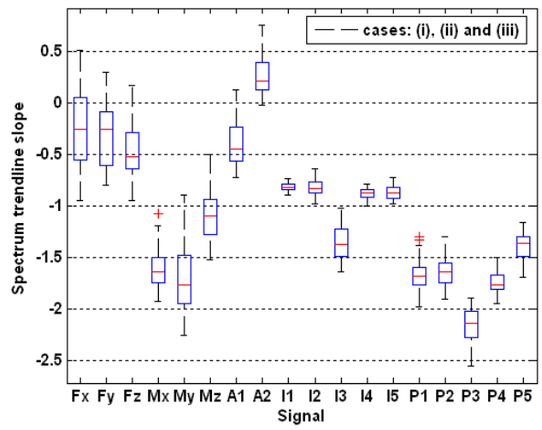

Fig. 14. Statistics of spectrum trendlines slopes for all the cases (*i, ii, iii*) using the thin and gross rods

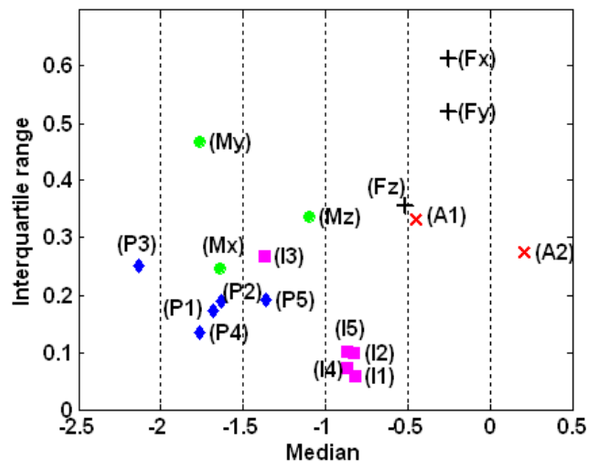

Fig. 15. IQR *versus* median for all the cases (*i, ii, iii*) using the thin and gross rods

3.4 Metrics in the time domain

Several indices can be used to evaluate the relashionship between the signal, including statistical, entropy and information theory approaches. These metrics are based on a bidimensional probability density function associated with the two signals $x_1(t)$ and $x_2(t)$ acquired in the same time interval and can be calculated according with the expression:

$$P(x_1,x_2)=\frac{\beta(x_1,x_2)}{\iint\beta(x_1,x_2)dx_1dx_2} \tag{2}$$

where β is the bidimensional histogram.

The marginal probability distributions of the signals $x_1(t)$ and $x_2(t)$ are denoted as $P(x_1)$ and $P(x_2)$, respectively. The expected values, $E(x_1)$ and $E(x_2)$, and the variances, $V(x_1)$ and $V(x_2)$, are then easily obtained.

The correlation coefficient R (Orfanidis, 1996) is a statistical index that provides a measurement of the similarity between two signals $x_1(t)$ and $x_2(t)$ and is define as

$$R(x_1,x_2)=\frac{E(x_1x_2)-E(x_1)E(x_2)}{\sqrt{V(x_1)V(x_2)}} \tag{3}$$

where $E(x_1x_2)$ is the joint expected value.

The mutual information (Shannon, 1948; Cover, 2006), or transinformation (Spataru, 1970) is the index that measures the dependence of two variables in the viewpoint of the information theory. The mutual information for the two signals $x_1(t)$ and $x_2(t)$ is:

$$I(x_1,x_2)=\log_2\frac{P(x_1,x_2)}{P(x_1)P(x_2)} \tag{4}$$

The average mutual information between the two signals is given by:

$$I_{av}(x_1,x_2)=\iint P(x_1,x_2)\log_2\frac{P(x_1,x_2)}{P(x_1)P(x_2)}dtdt \tag{5}$$

The entropy (Shannon, 1948) is a statistical measure of randomness. This index applied to the two signal $x_1(t)$ and $x_2(t)$ gives the join entropy (MacKay, 2003) between the two signal defined as:

$$H(x_1,x_2)=-\iint P(x_1,x_2)\log_2 P(x_1,x_2)dtdt \tag{6}$$

Figure 16 shows the squared correlation coefficient R^2 between the signals captured during the same impact trajectory, for an experiment in the case of (*i*) using the gross rod. The results obtain with R^2 are simetric relative to the diagonal formed by $R^2(x_i,x_j)$ for $i = j$, where the metric is maximum, as expected. To clearly visualize the results only one side is shown. The correlation between the same families of signals is higher than the correlation between different families. For example, the correlation between the currents and positions are low. The same occurs between the currents and the forces, moments and accelerations. It exists a

strong correlation between the positions and the forces, moments and accelerations that depends, as expected, on the trajectory.

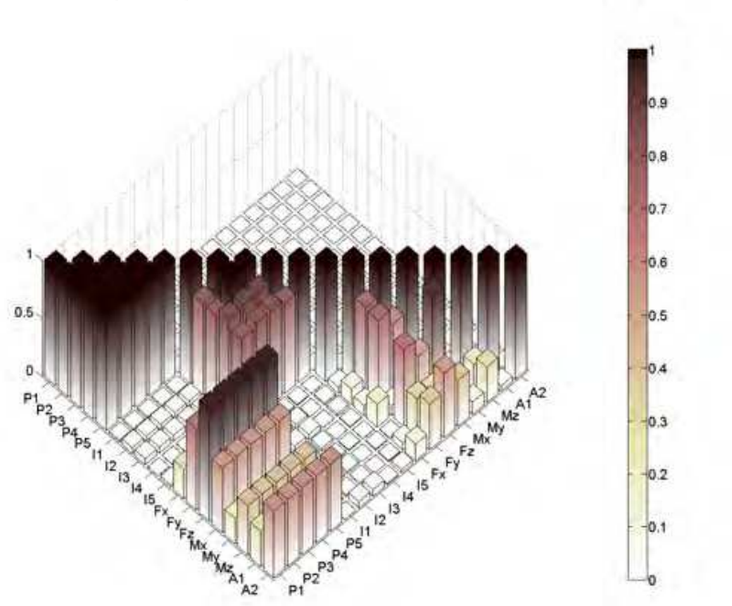

Fig. 16. Correlation between the signals for the case (*i*) using the gross rod

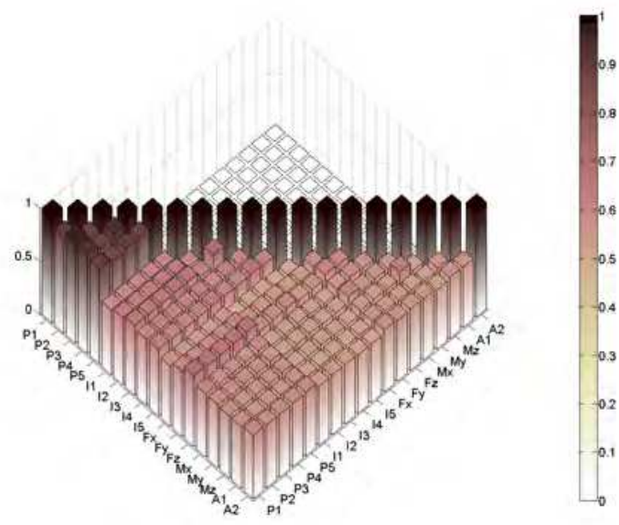

Fig. 17. Average mutual information between the signals for the case (*i*) using the gross rod

Figure 17 shows the average mutual information between the signals for the same experiment used previously for the correlation. Again the results obtain with $I_{av}(x_1, x_2)$ are simetric relative to the diagonal where the metric is maximum. Due to the same reason referred before only one side is shown. The values presented are normalized. The values of the index $I_{av}(x_1, x_2)$ between the positions are high.

Figure 18 shows a chart based on the entropy between the signals for the same experiment used previously for the other metrics. In fact, the values shown are proportional to the inverse of the index $H(x_1, x_2)$ due to the normalization used. Again, the values of this index between the positions are high.
The metrics shown in figures 16–18 were obtained for an experiment corresponding to one trajectory. In future this approach should be applied for all the thirteen trajectories referred before.

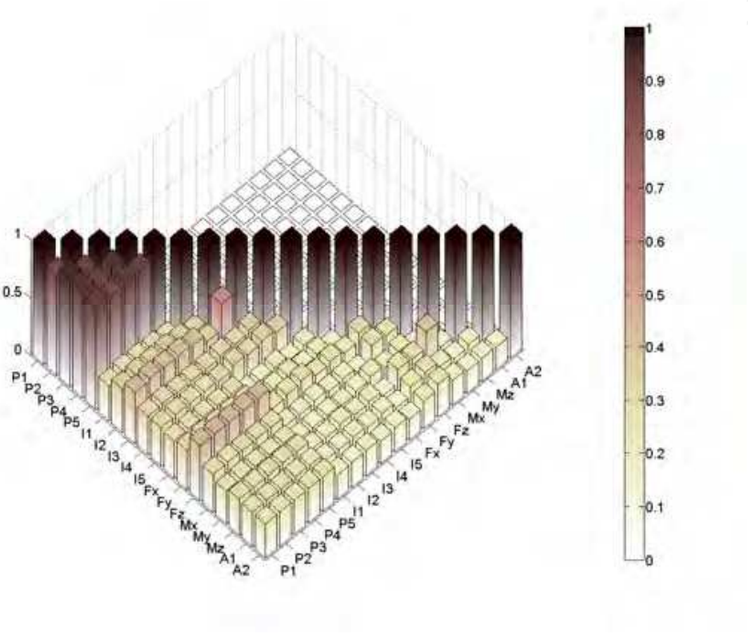

Fig. 18. Metric based on the entropy between the signals for the case (*i*) using the gross rod

4. Conclusion

In this paper an experimental study was conducted to investigate several robot signals. A new sensor classification strategy was proposed.
One of the adopted methodologies leads to arrange the robotic signals in terms of identical spectrum behavior, obtaining three groups of signals: the group of "positions and torques", the group of "currents" and the group of "forces and accelerations".
The other methodology is based on several metrics used to evaluate the relashionship between the signals in the time domain, namely the correlation, the average mutual information and the entropy. These indices revealed the hidden relationships between the signals.
The results merit a deeper investigation as they give rise to new valuable concepts towards instrument control applications. In this line of thought, in future, we plan to pursue several research directions to help us further understand the behavior of the signals.

5. Acknowledgment

The authors would like to acknowledge the GECAD unit.

6. References

Arampatzis, T. & S. Manesis (2005). A Survey of Applications of Wireless Sensors and Wireless Sensor Networks. *Proc. IEEE Int. Symp. on Intelligent Control*. pp. 719-724.

Cheekiralla, S. & W. Engels (2005). A functional taxonomy of wireless sensor network devices. *2nd International Conference on Broadband Networks IEEE*. - Vol. 2. - pp. 949-956. doi:10.1109/ICBN.2005.1589707.

Cover, T. & Thomas, J. (2006). *Elements of Information Theory*. John Wiley & Sons, ISBN-10 0-471-24195-4.

Esteban, J.; Starr, A.; Willetts, R.; Hannah, P. & Bryanston-Cross, P. (2005). A review of data fusion models and architectures: towards engineering guidelines. *Neural Computing & Applications*, Springer , London, 14(4):pp. 273–281.

Hackett, J. & Shah, M. (1990). Multi-sensor fusion: a perspective. *Proc. IEEE Int. Conf. on Robotics & Automation*, pages 1324–1330.

Henderson, T. & Shilcrat, E. (1984), E. Logical sensor systems. *J. of Robotic Systems*. - 2. - Vol. 1. - pp. 169-193.

Lima, M.; Machado, J. & Crisóstomo, M. (2005). Experimental Set-Up for Vibration and Impact Analysis in Robotics, *WSEAS Trans. on Systems*, Issue 5, vol. 4, May, pp. 569-576.

Lima, M.; Machado, J. & Crisóstomo, M. (2006). Windowed Fourier Transform of Experimental Robotic Signals with Fractional Behavior. *Proc. IEEE Int. Conf. on Computational Cybernetics*, August, Tallin, Estonia.

Lima, M.; Machado, J.; Crisóstomo, M. & Ferrolho, M. (2007). On the sensor classification scheme of robotic manipulators. *Int. Journal of Factory Automation, Robotics and Soft Computing - International Society for Advanced Research*, 3, pp.26–31, ISSN1828–6984.

Lima, M.; Machado, J. & Crisóstomo, M. (2007). Towards a sensor classification scheme of robotic manipulators, *CIRA- 7th IEEE International Symposium on Computational Intelligence in Robotics and Automation*, ISBN1424407907, Florida, USA, June,Jacksonville.

Luo, R. & Kay, M. (1990). A tutorial on multisensor integration and fusion. *IEEE 16th Annual Conf. of Industrial Electronics Society*, pp. 707–722, 1990.

MacKay, D. (2003). *Information Theory, Inference, and Learning Algorithms*. Cambridge University Press, August, ISBN 0521642981.

Michahelles, F. & Schiele, B. (2003). Sensing opportunities for physical interaction. *Workshop on Physical Interaction of Mobile HCI conference*, September, Udine, Italy

Orfanidis, S. (1996), *Optimum Signal Processing. An Introduction*. 2nd Edition, Prentice-Hall, Englewood Cliffs, NJ, 1996.

Robotec, E. (1996). *Scorbot ER VII, User's Manual*, Eshed Robotec, ISBN9652910333.

Shannon, C. (1948). A Mathematical Theory of Communication. *The Bell System Technical Journal*. July; October, Vol. 27, pp. 379-423; 623-656.

Spataru, Al. (1970). *Theorie de la Transmission de l'Information – Signaux et Bruits*. Editura technical, Bucarest, Roumanie.

White, R. M. (1987). A sensor classification scheme. *IEEE Trans. on Ultrasonics, Ferroelectrics and Frequency Control*, 34(2):124–126.

Robot Manipulators New Achievements

Edited by Aleksandar Lazinica and Hiroyuki Kawai

ISBN 978-953-307-090-2
Hard cover, 718 pages
Publisher InTech
Published online 01, April, 2010
Published in print edition April, 2010

Robot manipulators are developing more in the direction of industrial robots than of human workers. Recently, the applications of robot manipulators are spreading their focus, for example Da Vinci as a medical robot, ASIMO as a humanoid robot and so on. There are many research topics within the field of robot manipulators, e.g. motion planning, cooperation with a human, and fusion with external sensors like vision, haptic and force, etc. Moreover, these include both technical problems in the industry and theoretical problems in the academic fields. This book is a collection of papers presenting the latest research issues from around the world.

InTech Europe
University Campus STeP Ri
Slavka Krautzeka 83/A
51000 Rijeka, Croatia
Phone: +385 (51) 770 447
Fax: +385 (51) 686 166
www.intechopen.com

InTech China
Unit 405, Office Block, Hotel Equatorial Shanghai
No.65, Yan An Road (West), Shanghai, 200040, China
中国上海市延安西路65号上海国际贵都大饭店办公楼405单元
Phone: +86-21-62489820
Fax: +86-21-62489821

IntechOpen